

Determination of band-offset enhanced in InGaAsP – InGaAsP strained multiquantum wells by photocurrent measurements

Daive Tari, Milena De Giorgi, Roberto Cingolani, Ermanno Foti, and Claudio Coriasso

Citation: *Journal of Applied Physics* **97**, 043705 (2005); doi: 10.1063/1.1850602

View online: <http://dx.doi.org/10.1063/1.1850602>

View Table of Contents: <http://scitation.aip.org/content/aip/journal/jap/97/4?ver=pdfcov>

Published by the [AIP Publishing](#)

Articles you may be interested in

[Photocurrent spectroscopy of intersubband transitions in GaInAsN/\(Al\)GaAs asymmetric quantum well infrared photodetectors](#)

J. Appl. Phys. **112**, 084502 (2012); 10.1063/1.4754573

[Carrier relaxation dynamics in annealed and hydrogenated \(GaIn\)\(NAs\)/GaAs quantum wells](#)

Appl. Phys. Lett. **87**, 252111 (2005); 10.1063/1.2149154

[Optical properties of as-grown and annealed InAs\(N\)/InGaAsP strained multiple quantum wells](#)

J. Appl. Phys. **90**, 6230 (2001); 10.1063/1.1418422

[Measurement of AlInAsSb/GaInAsSb heterojunction band offset by photoluminescence spectroscopy](#)

Appl. Phys. Lett. **75**, 238 (1999); 10.1063/1.124334

[Investigation of photoluminescence and photocurrent in InGaAsP/InP strained multiple quantum well heterostructures](#)

J. Appl. Phys. **81**, 394 (1997); 10.1063/1.364070



Determination of band-offset enhanced in InGaAsP–InGaAsP strained multiquantum wells by photocurrent measurements

Davide Tari^{a)}

ISUFI, Istituto Superiore di Formazione Interdisciplinare, Nanoscience Dept., Via per Arnesano, 1-73100 Lecce, Italy

Milena De Giorgi and Roberto Cingolani

National Nanotechnology Laboratory of INFN, Dip. di Ing. dell'Innovazione, Università di Lecce, Via per Arnesano, 73100 Lecce, Italy

Ermanno Foti and Claudio Coriasso

Agilent Technologies Italia, TTC-Turin Technology Center, Via G. Reiss Romoli 274, 10148 Torino, Italy

(Received 12 March 2004; accepted 23 November 2004; published online 25 January 2005)

We experimentally determine the band offset of strain-compensated InGaAsP–InGaAsP multiquantum-well (MQW) heterostructures, emitting at 1.55 μm , that were grown by metal-organic chemical vapor deposition. A band offset value of about 56% is found for the conduction band, which is higher than the value reported for the unstrained structure. The temperature dependence of the photoluminescence intensity shows that the unipolar detrapping of carriers in such MQWs is more efficient than the thermal activation of excitons. © 2005 American Institute of Physics. [DOI: 10.1063/1.1850602]

In the last decade, the requirements for optical fiber communication systems have increased due to the continuous rise of long-haul and high bit rate technologies. For this reason, great efforts have been made to optimize the different components involved in the optical communication systems, such as optical modulators. High performance of external modulators in terms of spectral distortion, modulation frequency, contrast ratio, and polarization independence¹ are obtained by employing quantum-well (QW) heterostructures as the active material. In particular, InGaAsP–InGaAsP quantum-well structures are widely used due to: (i) Their relatively simple tuning between 1.3 and 1.55 μm , (ii) the large variation of absorption coefficient upon relatively low bias, and (iii) the possibility to achieve strain compensation between wells and barriers.² The last point is important because strain compensation enables the growth of relatively thick active layers with a high number of wells of larger thickness, resulting in a reduction of interface effects at the operating wavelength of the device.

A significant problem of InGaAsP QWs is optical saturation, which strongly depends on the generation rate, and on the escape, of carriers from the active region. InGaAsP unstrained heterostructures have a very large valence band discontinuity that prevents the escape of heavy holes from the QW under bias. This results in the accumulation of a positive charge density that screens the external electric field, and reduces the performances of the device.³ The escape of carriers can be enhanced by raising the temperature or the bias, or by a proper choice of the barrier thickness. However, it is the band offset that ultimately determines the performances of the device. In this letter, we study an InGaAsP–InGaAsP MQW heterostructure that was designed to have a low band

discontinuity, with the purpose of raising the optical power saturation and the modulation frequency of the device. The band offset of this heterostructure, determined experimentally by means of photocurrent measurements, is in good agreement with the theoretical estimation.

We investigate InGaAsP strain compensated multiquantum-wells, grown on InP substrate by metal-organic chemical vapor deposition (MOCVD). The structure consists of a 2 μm Se⁻ doped InP buffer on which it has been grown 250 Å of InGaAsP confining layer, followed by 8 periods of undoped InGaAsP (well width=80 Å)/InGaAsP (barrier width=65 Å) multiquantum-wells. Above these has been grown a 250 Å InGaAsP confining layer, 2 μm Zn doped InP layer and the structure is terminated with a 0.02 μm InP cladding layer. The structure has been designed to obtain a compression of about +0.6% in the well and a tensile strain of about -0.25% in the barrier. The compensation of the strain plays a fundamental role in the design of electroabsorption modulators, because it modifies both the band structure of the material and the optical and electronic properties.⁴ This results in a reduction of: (i) The valence band discontinuity, thus improving the modulation frequency and reducing the optical saturation; (ii) the chirp effect; and (iii) sensitivity to polarization.

The strain field of this heterostructure was calculated according to the strain model of Wang and Stringfellow.⁵ By defining the conduction band offset as

$$Q_c = \frac{\Delta V_e}{\Delta V_e + \Delta V_c}, \quad (1)$$

where ΔV_e and ΔV_c are the potential discontinuities of the conduction band and the heavy hole band, respectively, this model leads to an expected Q_c of 53% (an offset of 44% is expected for the unstrained structure). Using this value, the electronic structure is calculated by solving the Schrödinger

^{a)}Author to whom correspondence should be addressed; electronic mail: davide.tari@unile.it

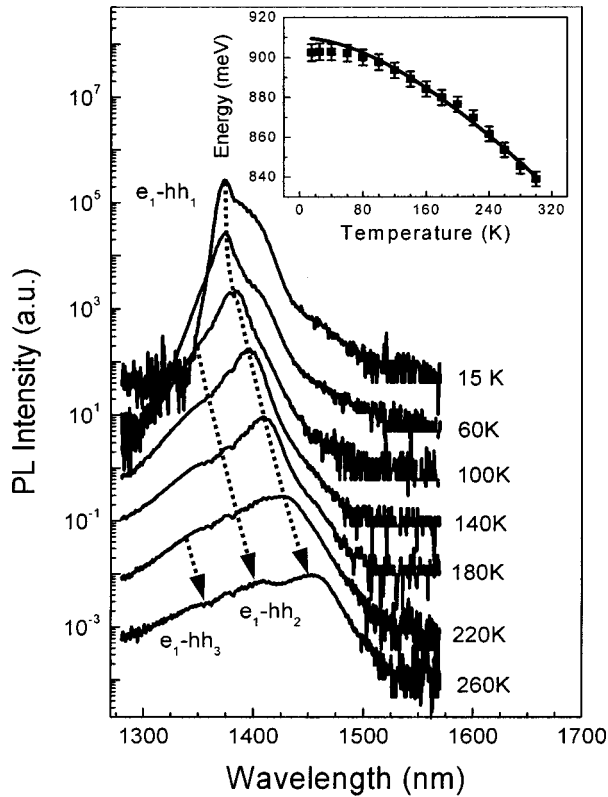


FIG. 1. Photoluminescence spectra of the InGaAsP–InGaAsP MQW at different temperatures (Argon laser, $\lambda=514.5$ nm). The inset shows the energy position of the e_1 – hh_1 transition vs temperature, fitted by the Varshni equation (solid line). The error bar indicates the spectral resolution of the system (50 cm monochromator and N_2 cooled Ge detector).

equation for a MQW system by means of the transfer matrix method (TMM). One confined state in the conduction band (e_1), and three heavy hole (hh_i with $i=1\div 3$) levels and one light hole (lh_1) level in the valence band are found in our structure.

Experimentally, the sample was studied by photoluminescence (PL) and by photocurrent (PC) measurements. In Fig. 1 we report the photoluminescence spectra in the temperature range between 15 and 300 K. The spectrum at 15 K shows the ground level e_1 – hh_1 excitonic transition at 1373 nm and a long tail (at around 1400 nm). At higher temperatures, the line shape of the tail does not change. We assign this tail to the transitions from localized defect states, which are ionized at $T > 90$ K. At high temperatures, due to thermal band filling, two other peaks can be identified in the fine structure (which is due to water absorption). These peaks are attributed to the e_1 – hh_2 transition (for $T > 140$ K) and to the e_1 – hh_3 transition (for $T > 220$ K). It is worth noting that the transition e_1 – hh_2 , which is forbidden at zero bias by the selection rules, can be observed here due to the presence of the internal electric field that breaks the flat band condition. The full width of half maximum (FWHM) of the PL spectra is estimated to be about 5.7 meV at 15 K and increases up to 16 meV at 300 K, reflecting the high quality of the quaternary multiple quantum well structure.^{6–8}

In the inset of Fig. 1, the peak energy of the e_1 – hh_1 transition vs temperature is shown. The experimental points follow the well-known Varshni equation:

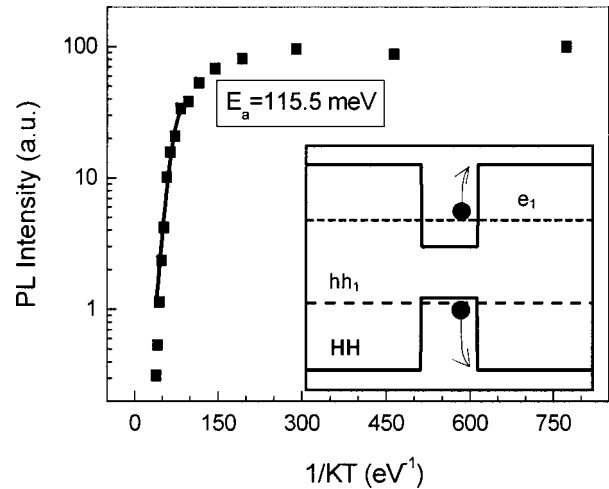


FIG. 2. Arrhenius plot of the e_1 – hh_1 transition. The estimated activation energy is about 115.5 meV. The inset shows the unipolar detrapping of carriers.

$$E_g(T) = E_g(0) - \frac{\alpha T^2}{\beta + T}, \quad (2)$$

where E_g is the energy gap of material, T the temperature, and α and β are Varshni's coefficients. β can be approximated as by the Debye temperature of the material.⁹

At low temperatures, the discrepancy between the values obtained from Eq. (1) at 0 K and the experimental data is due to the exciton localization at sites of compositional disorder. At higher temperatures the bound excitons start ionizing, and above 90 K the excitonic peak follows the Varshni equation.

Figure 2 shows the PL quenching of the dominant peak (e_1 – hh_1) when the temperature is increased to 300 K. From the Arrhenius plot (Fig. 2) we estimate that the activation energy of the PL quenching is around 115.5 meV, which is much lower than the calculated electron-hole confinement energy (about 192.5 meV), related at a theoretical band-offset of about 53%. The data indicates that the thermal quenching of the photoluminescence is due rather to the escape of the less-confined carrier species, which are the electrons. This mechanism thus confirms that in such heterostructures the unipolar detrapping of carriers is more efficient than the thermal activation of excitons (inset of Fig. 2). The small discrepancy between the estimated activation energy and the theoretical electron confinement energy can be explained taking into account two main factors: (i) As we will show in the following, the evaluated experimental band-offset is slightly higher (about $56 \pm 2\%$) and (ii) the exciton binding energy is not included in the strain model.

The determination of the precise spectral position of the different transitions is essential for determining the band-offset (Q_c) of such MQWs, which is a fundamental parameter for the correct design of a device at high bit-rate. The determination of the band discontinuity is generally obtained by an indirect approach. We performed photocurrent measurements at several applied voltages. From these measurements, we determined Q_c by considering the relation between the observed experimental energy transition in the

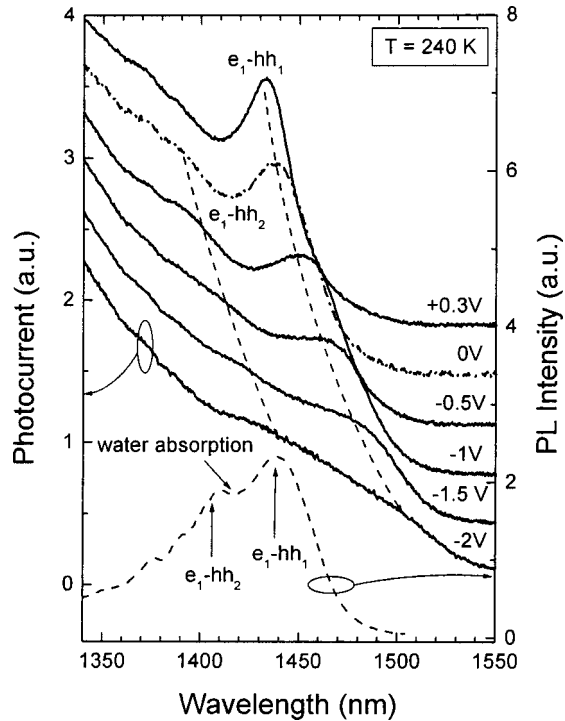


FIG. 3. Photocurrent spectra at 240 K for different applied voltages. The dashed curves show the evolution of the two optical transitions (e_1-hh_1 and e_1-hh_2) with the electric applied field. The PL spectrum, at the same temperature (dashed curve), clearly shows the e_1-hh_1 and e_1-hh_2 transitions.

photocurrent spectra, and the theoretical energy transition calculated at different band discontinuities and applied voltages.

Figure 3 shows the photocurrent spectra measured at 240 K at different applied voltages, and the corresponding PL spectra at this temperature. The two peaks observed in the spectra are attributed to the e_1-hh_1 and e_1-hh_2 transitions as confirmed by the theoretical calculation. In the PC spectra, the dominant transition e_1-hh_1 is evident for all applied voltages. On the other hand, the e_1-hh_2 transition becomes more evident for reverse bias. From such spectra we also see that by decreasing the external voltage, from +0.3 V to -2 V, two different effects are evident: (i) The red-shift of the optical transitions and (ii) a broadening of the peaks. The first effect is due to the quantum confined Stark effect (QCSE). By increasing the bias voltage, the energy separation between the levels is reduced resulting in a shift of the peaks towards a higher wavelength range. The Stark shift estimated for the transition e_1-hh_1 is about 65 nm. The broadening of the peaks is instead due to an accumulation of the wave functions of electrons and holes near the interfaces under reverse field. This results in an increased sensitivity to interface disorder. Since both carriers are highly confined by the barriers, the residual overlap of the wave functions spatial separation allows us to observe the ground level transition even at strong fields (up to 160 KV/cm for a bias of -2 V). For larger biases (>-2 V), the photocurrent spectra become flat and it is not possible to observe any transitions. The fit of the photocurrent spectra allows us to obtain the energetic position of both electronic transitions for different applied voltages, taking into account the excitonic effect and the Sommerfield factor under electric field.

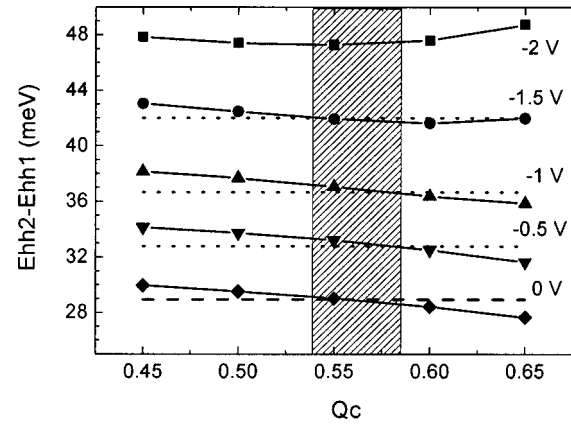


FIG. 4. Plot of the energy difference between e_1-hh_2 and e_1-hh_1 transitions as a function of Q_c for reverse bias at room temperature. The continuous curves are the theoretical ones, while the dotted (PC) and dashed (PL) curves are the experimental ones.

In Fig. 4, we plot the theoretical energy difference between the two observed transitions ($\Delta E = E_{e_1-hh_2} - E_{e_1-hh_1}$) as a function of Q_c for different reverse biases (solid curves in Fig. 4), calculated including the Stark and excitonic effects (the absolute values of the theoretical peak position are found to be 17 nm lower for both observed transitions). Q_c was determined from the intersection of these curves with the ΔE value measured experimentally in the photocurrent spectra (dotted curves of Fig. 4)¹⁰. It could also be possible to determine Q_c by using the values of the energy transitions obtained from the photoluminescence spectra. However, in our case, the PL spectra (Fig. 1) clearly show the e_1-hh_1 transition for all temperatures, while e_1-hh_2 and e_1-hh_3 transitions, due to water absorption, are too broad to obtain a fit with an acceptable error.

In Fig. 4, we see that the intersections between the values of ΔE obtained both experimentally and theoretically are not lined up along a unique value of band discontinuity, but they are distributed across a limited range of Q_c . This is due to the fact that the effect of the nonparabolicity of the bands has not been taken into account in the calculations. The value estimated for band discontinuity is $56 \pm 2\%$, which is in good agreement with the theoretical value ($\sim 54\%$). In Fig. 4 we also plot the ΔE value between e_1-hh_2 and e_1-hh_1 transitions, obtained by the deconvolution of the photoluminescence spectra at 240 K (dashed curve). At this temperature it is possible to clearly observe the e_1-hh_2 transition, which emerges from the water absorption. The intersection between this ΔE value and the theoretical curve at zero bias occurs at $Q_c = 55.5\%$, which confirms the value estimated from the PC measurements.

In conclusion, we have experimentally determined the band-offset of an InGaAsP-InGaAsP strained MQW, which is a fundamental parameter for the design of an electroabsorption modulator with high performance. The determined band-offset is in good agreement with the value estimated theoretically which confirms that the designed parameters of the structures are correct.

ACKNOWLEDGMENTS

This work is supported by Agilent Technologies. We thank G. Bastard, L. Manna, and Roman Krahné for useful discussions and P. Cazzato for valuable technical support.

¹R. W. Martin, S. L. Wong, R. J. Nicholas, K. Satzket, M. Gibbons, and E. J. Thrush, *Semicond. Sci. Technol.* **8**, 1173 (1993).

²F. Devaux, S. Chelles, A. Ougazzaden, A. Mircea, and J. C. Harmand, *Semicond. Sci. Technol.* **10**, 887 (1995).

³T. H. Wood, J. Z. Pastalan, C. A. Burrus, B. C. Johnson, B. I. Miller, J. L. deMiguel, U. Koren, and M. G. Young, *Appl. Phys. Lett.* **57**, 1081 (1990).

⁴T. Yamanaka, K. Wakita, and K. Yokoyama, *Appl. Phys. Lett.* **70**, 87

(1997).

⁵T. Wang and G. Stringfellow, *J. Appl. Phys.* **67**, 344 (1990).

⁶V. Swaminathan, G. L. Koos, and D. P. Wilt, *J. Appl. Phys.* **60**, 372 (1986).

⁷J. X. Chen, A. Z. Li, Y. Q. Chen, F. M. Guo, C. Lin, Y. G. Zhang, and M. Qi, *J. Cryst. Growth* **227-228**, 338 (2001).

⁸Y. C. Lee, H. T. Shu, J. L. Shen, K. F. Liao, and W. Y. Uen, *Solid State Commun.* **120**, 501 (2001).

⁹C. F. Li, D. Y. Lin, Y. S. Huang, Y. F. Chen, and K. K. Tiong, *J. Appl. Phys.* **81**, 400 (1997).

¹⁰M. Di Dio, M. Lomascolo, A. Passaseo, C. Gerardi, C. Giannini, A. Quirini, L. Tapfer, P. V. Giugno, M. De Vittorio, D. Greco, A. L. Convertino, L. Vasanelli, R. Rinaldi, and R. Cingolani, *J. Appl. Phys.* **80**, 482 (1996).